EDMS No. 456396

ORGANISATION EUROPEENNE POUR LA RECHERCHE NUCLEAIRE
EUROPEAN ORGANIZATION FOR NUCLEAR RESEARCH

Laboratoire Européen pour la Physique des Particules
European Laboratory for Particle Physics

TECHNICAL NOTE

CERN-SC-2004-24-RP-TN

COMPARISON OF THE SIMULATION AND MEASUREMENTS OF THE REPSONSE OF CENTRONIC HIGH-PRESSURE IONISATION CHAMBERS TO THE MIXED RADIATION FIELD OF THE CERF FACILITY

Christian Theis, Stefan Roesler and Helmut Vincke

Abstract

For the application of high-pressure ionisation chambers as radiation monitoring systems in a high-energy accelerator-specific environment, it is of great interest to know their response to mixed radiation fields. This Note describes the comparison of the simulation of such chambers of type IG5 by Centronic Ltd. to measurements previously performed in the mixed radiation field of the CERN-EU high-energy Reference Field (CERF) facility. Using calculated particle-specific response functions of these monitors it is studied how accurately their response in a mixed field of known particle and energy composition can be predicted by FLUKA Monte Carlo simulations.

CERN, Geneva, Switzerland
06.05.2004

1 INTRODUCTION

Radiation fields typically encountered at an high-energy accelerator show a composition of many different particle types over a wide range of energy. These fields are quite different from environments in which radiation monitoring systems are normally used like at nuclear power plants. Therefore, it is of vital importance to study the behaviour of such monitoring devices in mixed fields in order to assess their suitability for radiological surveillance systems at an accelerator.

For the Large Hadron Collider (LHC) a modern state of the art Radiation Monitoring System for the Environment and Safety (RAMSES) will be implemented using different kinds of radiation detectors. Presently it is foreseen to install argon- and hydrogen-filled ionisation chambers in areas where dose is due to neutrons, photons and various charged particles. Because of the fact that IG5 ionisation chambers, manufactured by Centronics Ltd., are currently used at the Super Proton Synchrotron (SPS) and its respective experimental areas, it stands to good reason to investigate their applicability for the RAMSES project.

Until now the calibration of these monitors has been performed using photon and neutron calibration sources at CERN's calibration laboratory. As a result factors for a neutron spectrum up to 11 MeV and mono-energetic photons are obtained. This procedure neglects the sensitivity of these devices to other particles and furthermore implies that the calibration factor is not a function of the particle energy. In consideration of their application in mixed radiation fields FLUKA [1,2] Monte Carlo simulations have been performed to calculate response functions for various particle types over a wide range of energies [3,4]. In order to validate the simulation results comparisons to calibration measurements using mono-energetic neutrons [4] and photons [5] at specific energies have been performed.

Following the calibration in mono-energetic fields first tests in a mixed radiation environment were performed at the CERN-EU high-energy Reference Field (CERF) facility [6,7]. Several chambers were placed at different exposure locations to perform measurements of the response as a function of the beam intensity. This Note describes the simulations resembling the settings of the CERF experiments. Consequently the measurement results were used to benchmark these simulations of the response of the monitors in a mixed field of known particle and energy composition.

2 FLUKA SIMULATIONS OF THE MIXED RADIATION FIELD AT CERF

Results obtained with Monte Carlo transport codes carry uncertainties which depend on the physical and geometrical models, as well as the number of histories followed in the simulation (statistical uncertainties). The approximations assumed in the calculations usually constitute a compromise between the level of complexity of the geometrical setup and the statistical uncertainties. Hence, they have to be evaluated on a case-by-case basis. Often the answer to a certain problem can be obtained already with simplified setups,

yielding results with a high statistical accuracy within a reasonable CPU-time. Therefore, the calculations discussed in the following were performed using a detailed geometry model of the CERF experimental area [8] as well as an extremely simplified model (see Appendix for a comparison of the particle fluences yielded by the two different setups). As can be seen from Figures 1 and 2 the complexity in the latter was drastically reduced to a copper target surrounded by a cylindrical concrete shielding, however, retaining the actual dimensions, such as the thickness of the shielding (80 cm), as well as the distance between the beam axis and the shielding. In order to simulate the experimental conditions as accurately as possible a source routine was implemented to sample the spatial distribution of a beam with a momentum of 120 GeV/*c*, as a two-dimensional Gaussian with a standard deviation of 1.3 cm in x - direction and 1.0 cm in y – direction respectively. Furthermore, the particle composition was sampled corresponding to a mixed beam of 61% pions, 35% protons and 4% kaons. Regarding the beam alignment the actual CERF setup was implemented in the accurate geometry with the target- and the beam-axis directed slightly towards the measurement locations (see below). For simulations applying the simplified geometry a similar mixed beam was used, however the Gaussian beam profile was replaced by a pencil beam. In addition the beam axis coincided with the symmetry axis of the cylinders.

As a result of the measurements the net charge produced by the various particles traversing the active volume of the chamber was obtained. In order to acquire a comparable quantity from the simulation the fluence spectra at the respective measurement locations (see Table 1) were calculated. Graphical representations of the detailed geometry setup and descriptions of the CERF reference locations can be found in Ref. [7]. The fluence spectra were scored in air-volumes of a size of 50 cm x 20 cm x 20 cm at the exposure locations. In the case of the simplified geometry the particle fluence spectra were obtained in a 20 cm thick cylindrical binning outside the concrete shell, which corresponds approximately to the diameter of the ionisation chambers.

Table 1 *Exposure locations used for the IG5 chambers at CERF. See Ref. [7] for further details. The abbreviations, as given in the first column, will be used throughout the Note.*

Abbreviation	Description
CS2	Concrete side position 2
CS-50U	Concrete side position, rear of the monitor located 50 cm upstream of the target front face
CT4	Concrete top position 4
CT6/T10	Boundary of concrete top position 6 and 10
I1	Inside position 1: head of the monitor located 100 cm downstream of the target front face at 50 cm lateral distance from the beam axis
I2	Inside position 2: head of the monitor located 275 cm downstream of the target front face at 50 cm lateral distance from the beam axis

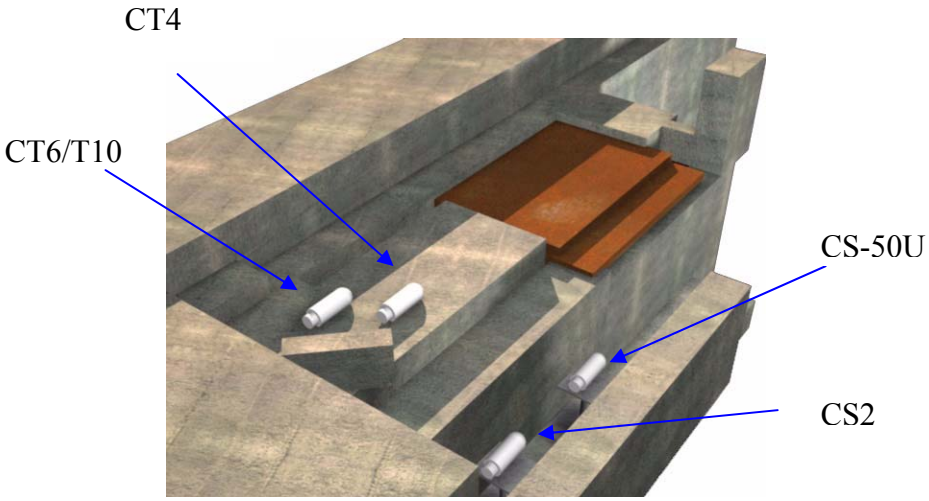

Figure 1 *Detailed geometry of the CERF experimental area used for the FLUKA calculations.*

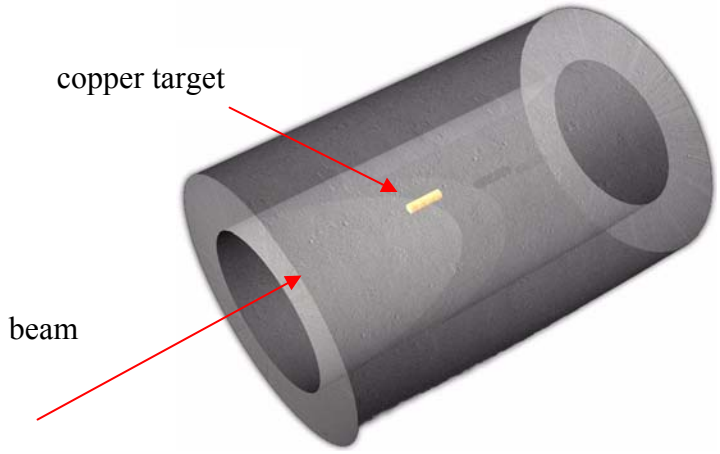

Figure 2 *Extremely simplified geometry of the CERF area used for comparisons with the detailed model.*

Due to particle attenuation by the concrete shielding biasing techniques in the particle transport were applied in order to obtain results with high statistical significance within a reasonable amount of CPU-time. Thus, the shielding was split into subregions to which region importance factors were assigned. The values were selected corresponding to multiples of the inverse of the hadronic attenuation factor for concrete, increasing towards the outside of the shield. As a consequence particle splitting at each boundary crossing was introduced according to the ratio of importances of adjacent regions. The weight of the split particles was adjusted automatically in order to account for the introduced bias. The aim of this simple biasing approach is to keep the particle population constant in the Monte Carlo simulation. For the calculations performed for the positions inside the shielding of the detailed geometry further CPU-time reduction was obtained by adjusting the material settings of specific regions. Because of the fact that particle histories traced, *e.g.*, inside the beam dump downstream of the target or outside the shielded cave will not contribute significantly to the particle fluence spectra near the target, these regions were assigned to be “black-hole”. Consequently, all particles entering such regions are not traced anymore.

Response functions for photons, neutrons, protons, pions and electrons have already been calculated for the argon- as well as for the hydrogen-filled chamber [4]. Convoluting the calculated response functions of the respective particles, expressed in terms of charge per unit fluence, with the corresponding particle fluence spectra yields the amount of created charge within the active chamber volume for each exposure location. Consequently, the total amount of produced charge per beam spill can be obtained by summation over all considered particle types and normalization to the number of particles per spill ($2.3 \times 10^4 \pm 10\%$). This number can be directly compared to the experimental values. For the positions outside the contribution of electrons to the total response is of minor importance an can be neglected. Due to the significant fluence of high-energy electrons inside the shielding electron response functions were also taken into account in the calculation of the created charge for the positions I1 and I2. The calculation of the response functions was performed for discrete energy values only, which differ from the energy bin structure of the obtained spectra, with the exception of low-energy neutrons. Therefore, interpolation was necessary, which was performed using custom-written software that provided either linear or constrained cubic spline interpolation of the response functions as well as subsequent convolution. Tests applying both interpolation methods showed that the difference in the results is negligible in comparison to the statistical uncertainty. For all calculations cubic-spline interpolation was applied.

The electromagnetic cascade was simulated in detail down to kinetic energy thresholds of 200 keV and 100 keV for electrons/positrons and photons, respectively. Due to the fact that photons with energies higher than 10 MeV were expected, which is the initial upper limit for which the response to photons was calculated, the respective response simulations discussed in Ref. [4] were extended up to 1 GeV. Generally, the scoring of hadrons was performed in a seperate run with the electromagnetic cascade turned off, which allowed for using a larger number of simulated histories within a reasonable amount of CPU-time. In the case of the detailed geometry 75000 source particles were traced while scoring the hadronic fluence spectra. Using the simplified cylindrical model the number of histories was reduced to 25000 particles. 5000 source particles were tracked for the calculation of the photon and electron fluence spectra in both geometries.

3 COMPARISON OF THE MEASUREMENTS AND THE SIMULATION

The calculation of the particle fluence spectra and the created net charge was performed for all exposure locations given in Table 1. In order to illustrate the obtained spectra the results for the location CT6/T10 and I1 are given in Figure 3 and 4, respectively. The shown spectra are based on calculations using the detailed geometry model of the CERF facility.

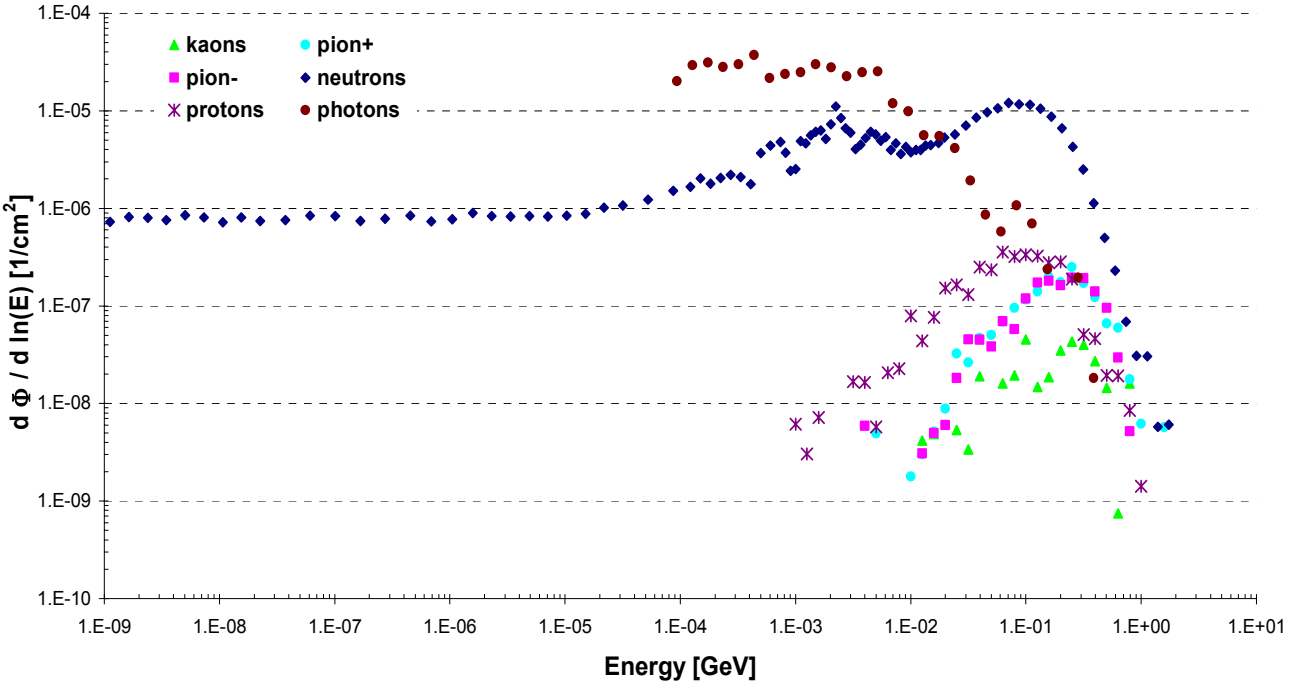

Figure 3 *Calculated particle fluence spectra per primary particle at the position CT6/T10 for various particles (lethargy representation).*

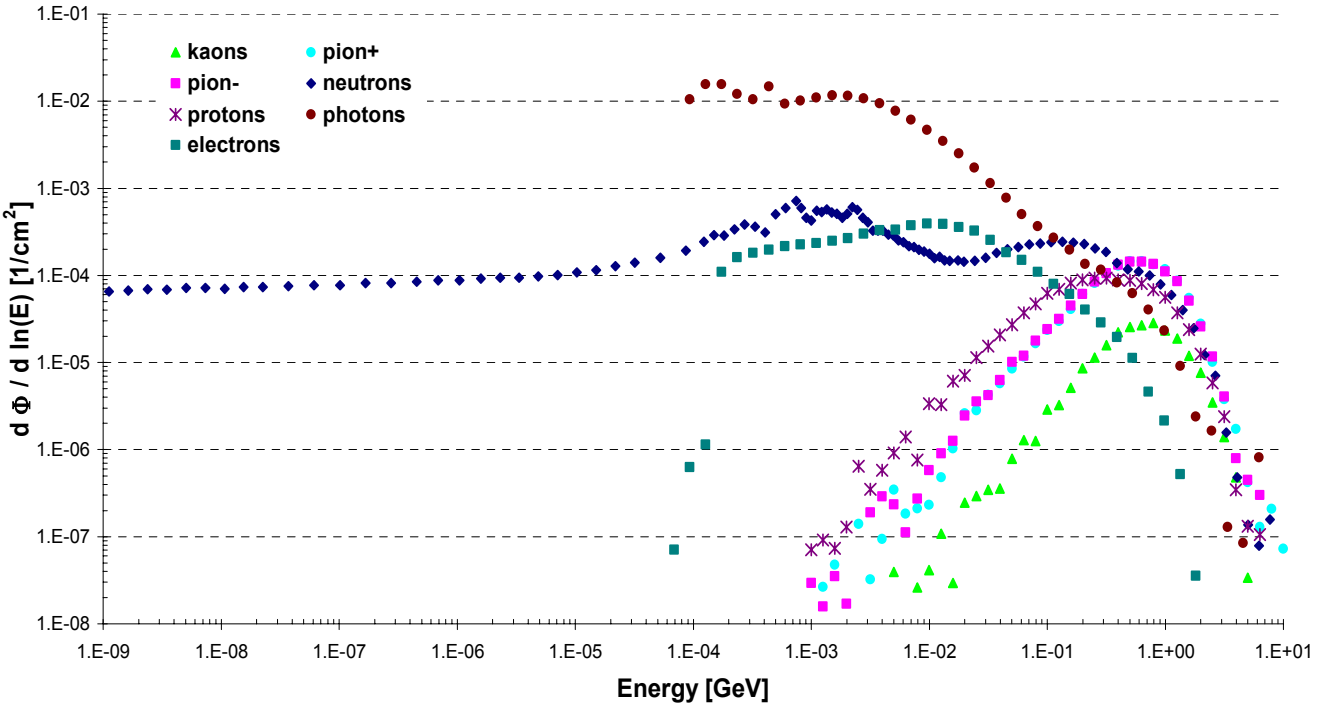

Figure 4 *Calculated particle fluence spectra per primary particle at the position I1 for various particles (lethargy representation).*

As can be seen from Figure 3 the predominant particles at the CT6/10 position are neutrons and photons, whereas, as shown in Figure 4, inside the shielding significant electron fluence can be observed. The contributions given in Tables 2 and 3 were acquired by folding calculated response functions [4] with particle fluence spectra obtained with the detailed geometry. Comparing the argon- to the hydrogen-filled chamber one finds that for positions outside the shielding protons and charged particles constitute the main contribution to the total response of the former type, whereas for the latter neutrons are generally the predominant contributors. At locations inside the shield (I1 and I2) the electromagnetic cascade, originating mainly from π^0 decays, dominates the created charge produced within the active volume for both detector types. Furthermore, in comparison to position I1 harder spectra are notable at position I2 (see Appendix), which is due to the forward peaked electromagnetic cascade.

Table 2 *Fractions of the total net charge created by various particle types at various exposure locations for an argon-filled chamber.*

Position	neutrons	protons	π+	π -	photons	electrons
CS2	0.303 ± 0.013	0.226 ± 0.037	0.067 ± 0.017	0.060 ± 0.015	0.344 ± 0.041	-
CS-50U	0.354 ± 0.032	0.145 ± 0.073	0.007 ± 0.006	0.026 ± 0.020	0.468 ± 0.123	-
CT4	0.346 ± 0.016	0.199 ± 0.039	0.033 ± 0.012	0.027 ± 0.010	0.395 ± 0.053	-
CT6/T10	0.297 ± 0.011	0.245 ± 0.033	0.059 ± 0.012	0.050 ± 0.011	0.350 ± 0.036	-
I1	0.027 ± 0.001	0.139 ± 0.004	0.096 ± 0.002	0.089 ± 0.002	0.459 ± 0.006	0.190 ± 0.007
I2	0.025 ± 0.001	0.102 ± 0.008	0.151 ± 0.007	0.131 ± 0.007	0.346 ± 0.007	0.246 ± 0.018

Table 3 *Fractions of the total net charge created by various particle types at various exposure locations given for a hydrogen-filled chamber.*

Position	Neutrons	Protons	π+	π -	photons	electrons
CS2	0.635 ± 0.040	0.141 ± 0.023	0.025 ± 0.006	0.025 ± 0.006	0.174 ± 0.021	-
CS-50U	0.746 ± 0.086	0.071 ± 0.035	0.002 ± 0.002	0.008 ± 0.006	0.173 ± 0.046	-
CT4	0.654 ± 0.040	0.124 ± 0.025	0.012 ± 0.010	0.011 ± 0.010	0.198 ± 0.027	-
CT6/T10	0.589 ± 0.030	0.168 ± 0.024	0.024 ± 0.005	0.023 ± 0.010	0.196 ± 0.020	-
I1	0.114 ± 0.005	0.139 ± 0.004	0.064 ± 0.002	0.064 ± 0.002	0.415 ± 0.006	0.174 ± 0.007
I2	0.138 ± 0.007	0.106 ± 0.009	0.102 ± 0.005	0.096 ± 0.005	0.328 ± 0.007	0.231 ± 0.017

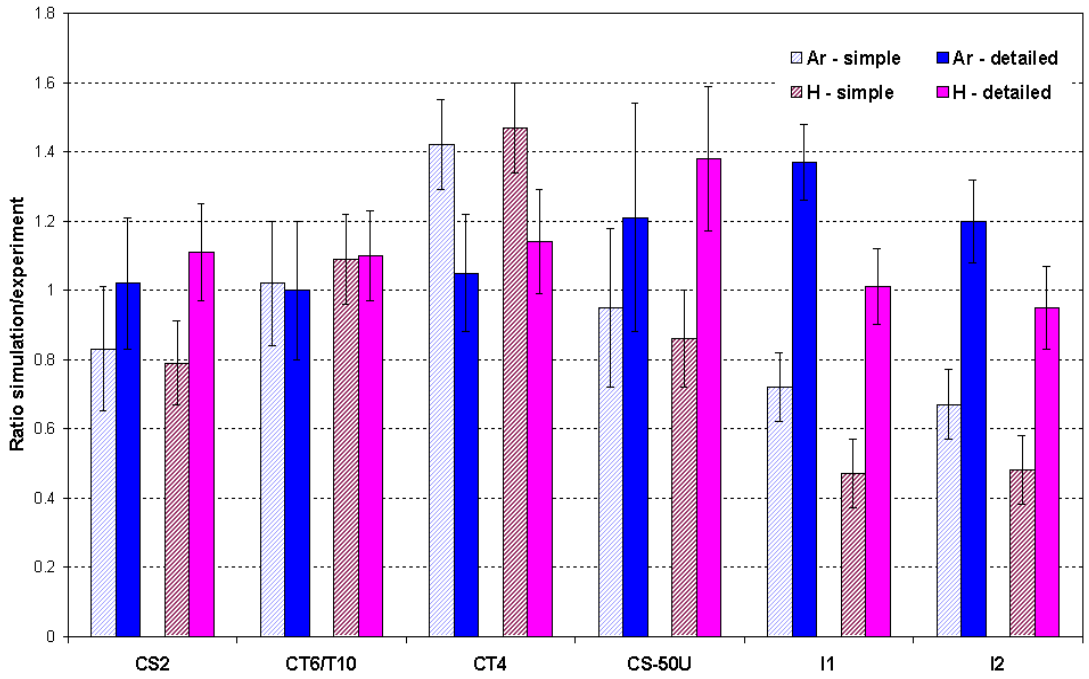

Figure 5 *Ratio of the calculated and the measured net charge for an argon-filled and a hydrogen-filled IG5 ionisation chamber using either a simplified or a detailed geometry model in the simulation.*

The ratio of the calculated and the measured charge, using either the simplified or the detailed geometry model, are given in Figure 5. As can be seen, for the exposure location CS2 the calculated charge using the simplified model is lower than the measured value, whereas good agreement is found with the detailed geometry. Considering the ratio for position CT6/T10, which should be comparable to location CS2, one finds good agreement for both monitor types and both geometry models. Thus, for position CS2 the deviation of the simulated from the measured values using the cylindrical geometry can be explained by the negligence of the additional shielding between the measurement locations and the CERF control room. This result is in accordance with the effect that the measured net charge at the CS2 location is larger than the values obtained at position CT6/T10, although comparable results were expected at first [7].

The comparison for the reference position CT4 shows that the cylindrical approximation is not correct in this case, as it yields a lower fluence spectrum due to the larger effective thickness of the shielding which has to be traversed. However, this artefact is resolved by the use of the detailed geometry. Considering the findings for the upstream position CS-50U one observes slight underestimation with the cylindrical and overestimation with the accurate geometry implementation of the experimental area. This is especially true for the hydrogen-filled chamber, although the simulation results with the accurate model show systematic overestimation for this monitor type for all outside exposure locations. A possible explanation of this effect could be the simplification of scoring the particle fluence spectra in air-filled volumes and folding with response functions for lateral irradiation, whereas in reality the majority of the particles has to traverse the base plate of the chamber before reaching the active volume. Considering the

fact that the response decreases slightly for irradiation from the rear [7], this could explain the overestimation yielded by the simulations.

The results found for the measurement locations inside the shielding have to be considered with care, as only one chamber of each monitor type was used for the measurements due to a lack of beam-time. Thus, no relevant statistical information is available that could help to estimate the influence of the chamber production series on the results. As can be seen from Figure 5 a deviation of simulated and the measured net charge can be observed for the inside positions using the simplified geometry. This can be explained by the assumption of the chamber axis and the beam alignment being parallel, whereas in reality the target- and the beam-axis are directed slightly towards the monitor. However, the result of the calculations can be improved by the application of the detailed geometry, taking the actual beam alignment into account. Consequently good agreement for the hydrogen-filled monitor is found, whereas the simulation of an argon-filled monitor shows overestimation. For all these comparisons the validity of a constant *W*-factor was assumed which may account for the observed discrepancies between the results of simulation and experiment. Furthermore, the measurements inside the shielding should be repeated with different chambers for verification.

7 RESULTS & CONCLUSIONS

For the application of ionisation chambers in a high-energy accelerator specific environment the response to mixed radiation fields is of great interest. Consequently, in addition to previous simulations of the monitor response to specific mono-energetic particle types, calculations for radiation fields of mixed particle and energy composition were performed. These simulations resembled the actual setup of experiments that were accomplished at CERF during July and August 2003. Subsequently the measured results were used to benchmark the calculations.

The FLUKA Monte Carlo transport code was used to score particle fluence spectra using a detailed geometry model of the CERF experimental area, as well as a very simplified cylindrical model. The application of these two different geometry setups allowed for evaluating a degree of simplification that will still yield comparable results with respect to the performed measurements.

Convoluting the particle fluence spectra that were scored at the locations used during the experiments, with the previously calculated and interpolated particle response functions yields the total amount of created charge. Scaling this result with the number of particles per beam spill ($2.3 \times 10^4 \pm 10\%$) one obtains the produced net charge per spill which can be directly compared to the measurements for benchmarking purposes. As a result it can be observed that for the simplified geometry good agreement is found for the CT6/T10 position, whereas all other positions show deviations for both chamber types. The discrepancy of the CS2 location is due to the fact that the additional shielding wall in the direction of the CERF control room is not taken into account. Thus, the contribution of scattered particles, that is due to these concrete blocks, is neglected and therefore underestimation can be observed. This effect vanishes using the detailed geometry model. For all other positions the assumption of a cylindrical geometry is quite coarse and results

in deviations because in comparison to the more accurate geometry implementation lower fluence spectra are obtained. Generally, good agreement is found with the application of the detailed geometry for all outside positions. However, systematic overestimation (approximately 10%) can be observed for the hydrogen-filled chamber.

Considering the results of the comparisons between calculations and measurements for the inside positions it is visible that the beam alignment in the simulation the deviates from the experimental setup has a rather significant impact. Performing the same simulations using a detailed geometry model and taking the realistic beam alignment into account, good agreement was found for the hydrogen-filled chambers for both locations inside the shielding. For the argon-filled devices, which are more sensitive to photons and electrons than the hydrogen-filled monitors, the simulations showed overestimation of the response. However, it should be kept in mind that the measurement results were obtained with one chamber of each type only. Additionally, for all simulations a constant *W*-factor was assumed which may also account for a possible deviation of simulated and measured values. Generally, good agreement was found using a detailed model of the experimental area, whereas simplifications should be done with care only. The negligence of essential details like, *e.g.*, additional shielding will have a significant impact on the results, although geometric simplification yields the requirement for less CPU-time. For practical purposes one has to decide the level of implemented details on a case-by-case basis, keeping the possible effect on the results in mind.

ACKNOWLEDGEMENTS

We would like to thank D. Forkel-Wirth for stimulating discussions and her support which allowed for the implementation of a new data acquisition system used for the measurements. We would also like to thank N. Aguilar, P. Carbonez, S. Mayer, M. Pangallo, D. Perrin, and M. Renou for their help in setting up the experiments used to benchmark the simulation results.

REFERENCES

1 A. Fasso', A.Ferrari, P.R. Sala, *Electron-photon transport in FLUKA: status*, Proceedings of the MonteCarlo 2000 Conference, Lisbon, October 23-26 2000, A.Kling, F.Barao, M.Nakagawa, L.Tavora, P.Vaz - eds., Springer-Verlag Berlin, p.159-164 (2001)

2 A. Fasso', A. Ferrari, J. Ranft, P. R. Sala, *FLUKA: Status and Prospective for Hadronic Applications*, Proceedings of the MonteCarlo 2000 Conference, Lisbon, October 23-26 2000, A.Kling, F.Barao, M.Nakagawa, L.Tavora, P.Vaz - eds. , Springer-Verlag Berlin, p.955-960 (2001)

3 T. Otto, *Preliminary simulation results for the sensitivity of Centronic high-pressure ionisation chambers*, CERN Technical Note TIS-RP-TN-2002-011 (2002)

4 C. Theis, M. Rettig, S. Roesler, H. Vincke, *Simulation of the response functions of Centronic high-pressure ionisation chambers using FLUKA*, CERN Technical Note SC-2004-23-RP-TN (2004)

5 A. Hess, *Détermination de la réponse de chambres d'ionisation prévues pour la surveillance du LHC*, CERN/Haute Ecole Specialisee du Suisse Occidentale (2002)

6 A. Mitaroff, M. Silari, *The CERN-EU high-energy Reference Field (CERF) facility for dosimetry at commercial flight altitudes and in space,* Radiation Protection Dosimetry 102, p. 7-22 (2002)

7 C. Theis, N. Aguilar, M. Pangallo, D. Perrin, M. Renou, S. Roesler, H. Vincke, *Centronic high-pressure ionisation chambers measurements in the mixed radiation field of the CERF facility*, CERN Technical Note TIS-RP-TN-2003-024 (2003).

8 H.Vincke, *Benchmarking o fthe simulation of the ATLAS hall background*, Ph.D. Thesis, CERN / Technische Universitaet GRAZ, (2000).

APPENDIX

Particle fluence spectra

The Figures 6 - 13 show the fluence spectra per primary particle of the considered particle types for the various CERF measurement locations that were used in the simulation. The spectra were obtained using the detailed geometry model.

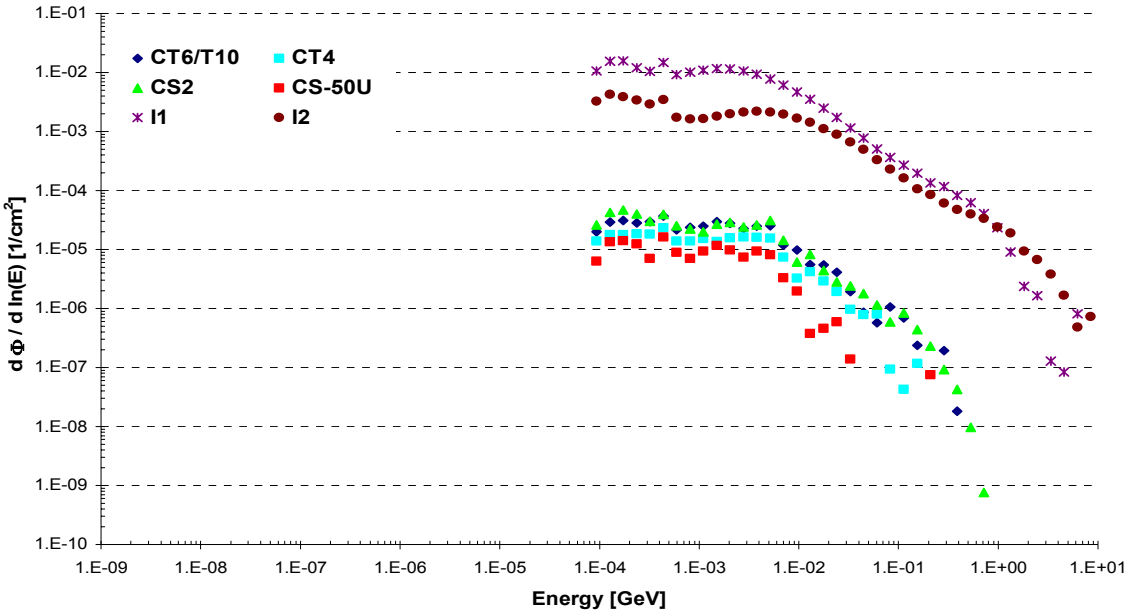

Figure 6 *Photon fluence spectra for various measurement locations at CERF (lethargy representation). The error bars were omitted for clarity.*

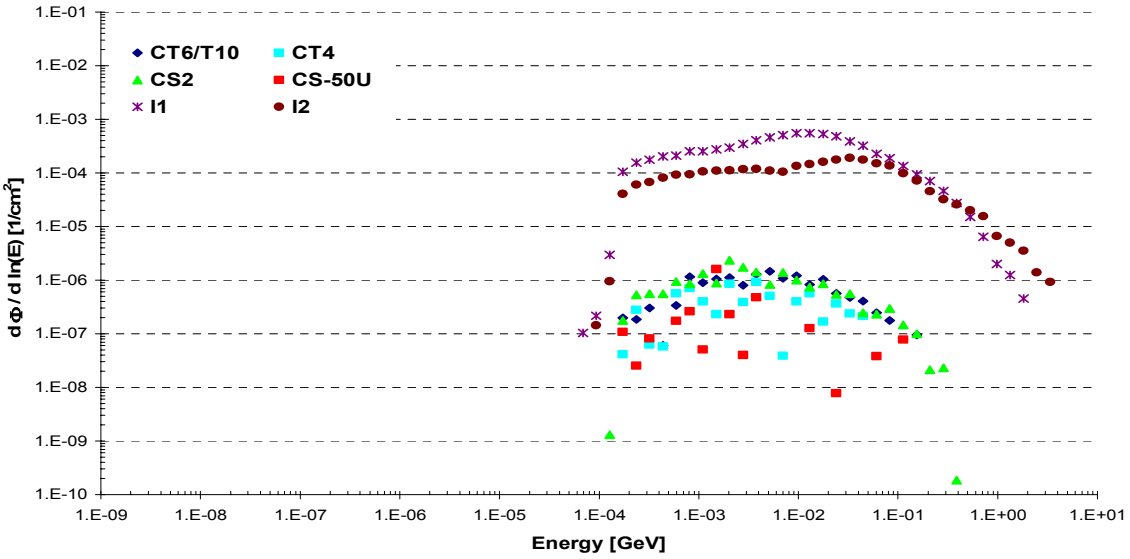

Figure 7 *Electron fluence spectra for various measurement locations at CERF (lethargy representation). The error bars were omitted for clarity.*

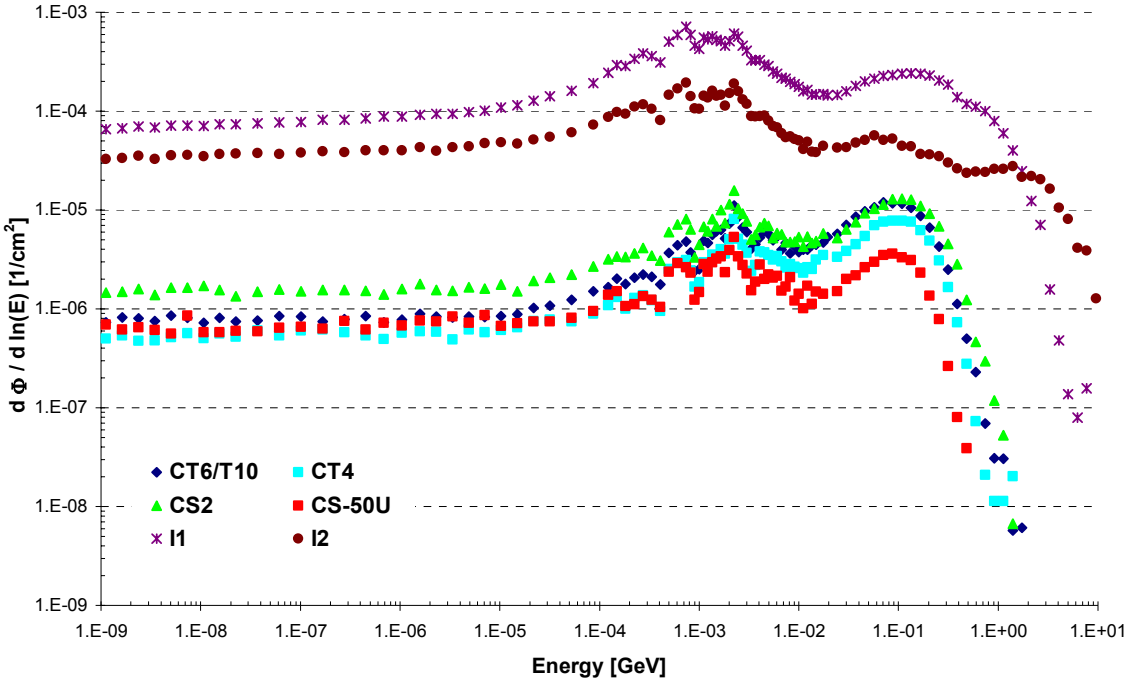

Figure 8 *Neutron fluence spectra for various measurement locations at CERF (lethargy representation). The error bars were omitted for clarity.*

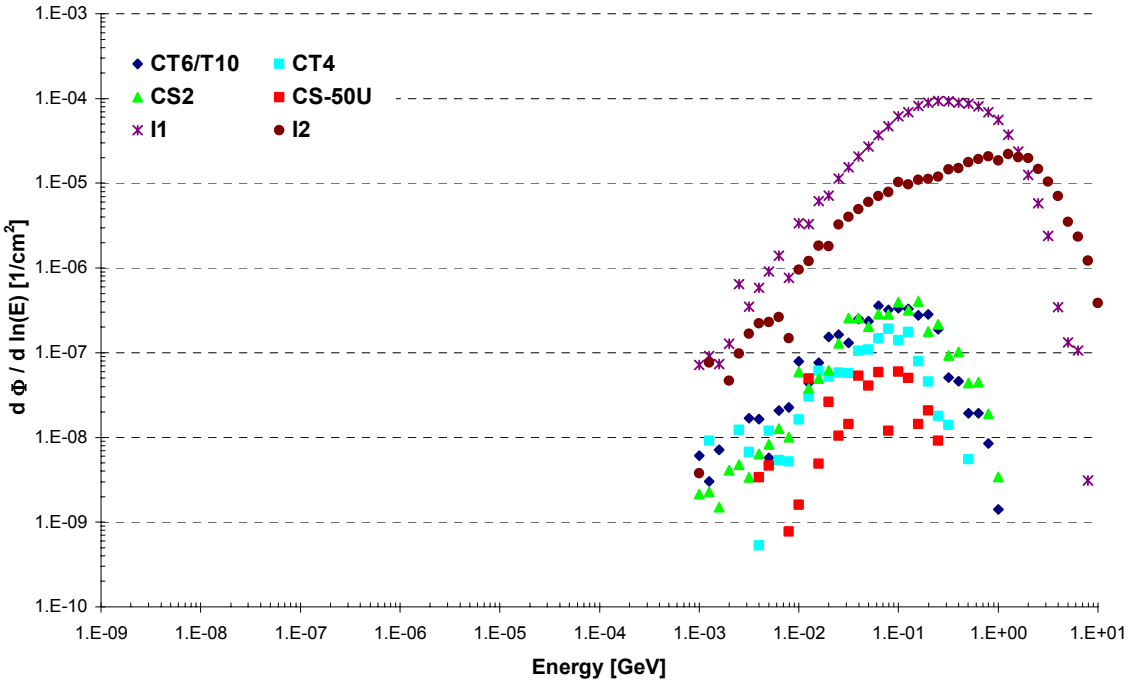

Figure 9 *Proton fluence spectra for various measurement locations at CERF (lethargy representation). The error bars were omitted for clarity.*

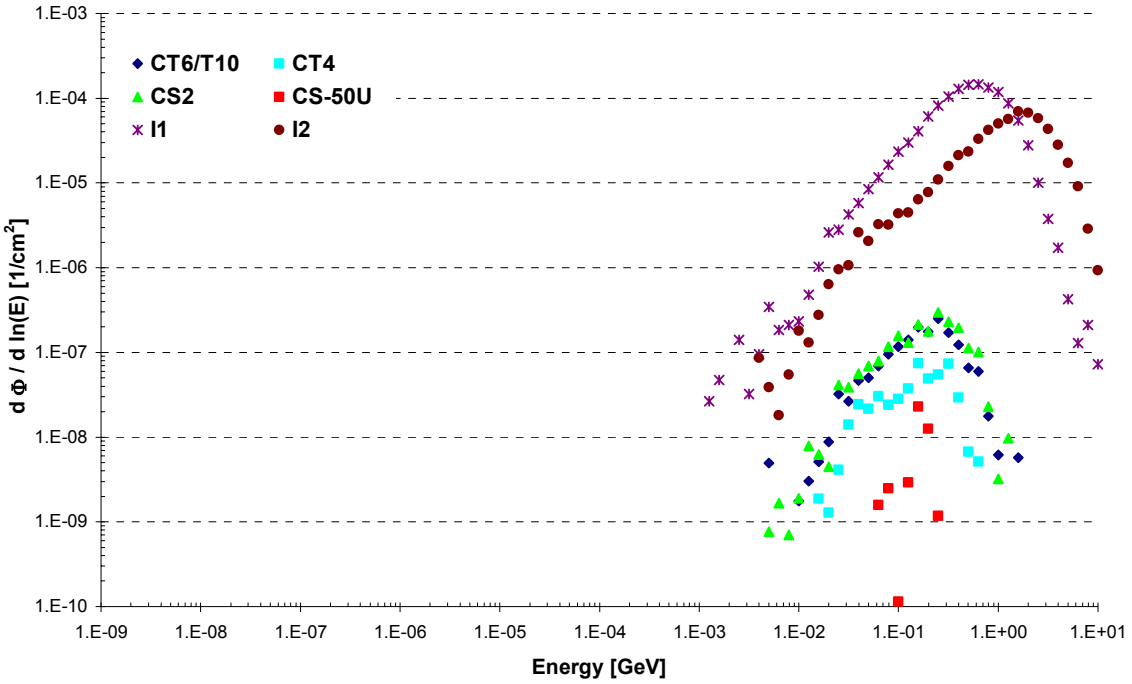

Figure 10 π^+ *fluence spectra for various measurement locations at CERF (lethargy representation). The error bars were omitted for clarity.*

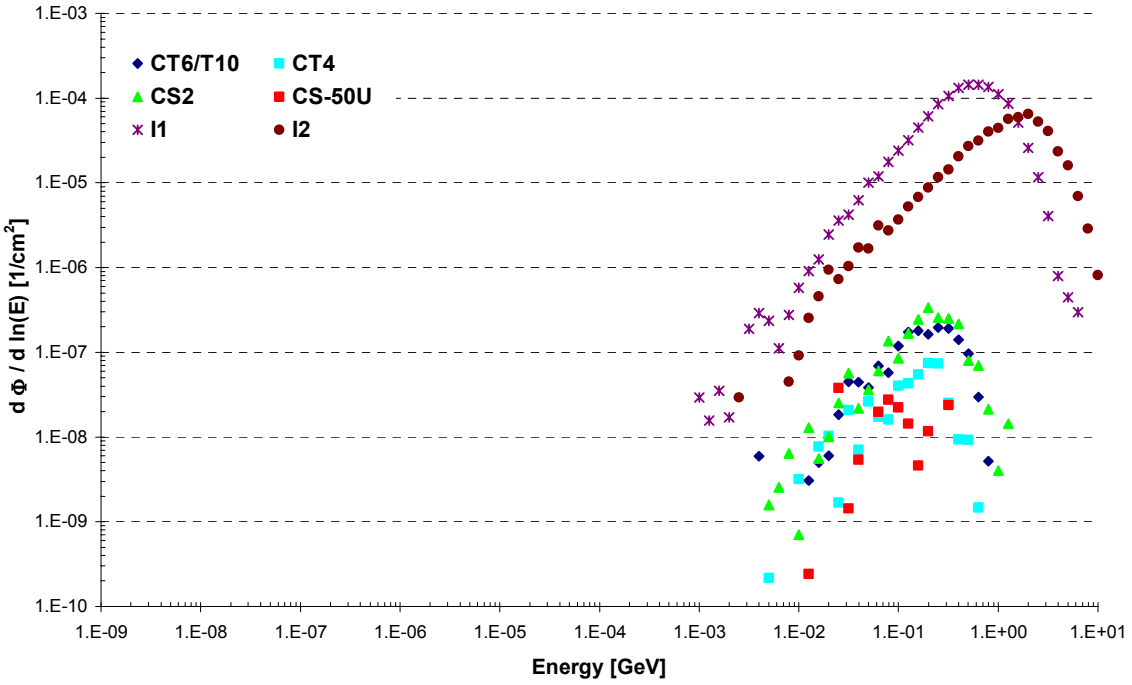

Figure 11 π^- *fluence spectra for various measurement locations at CERF (lethargy representation). The error bars were omitted for clarity.*

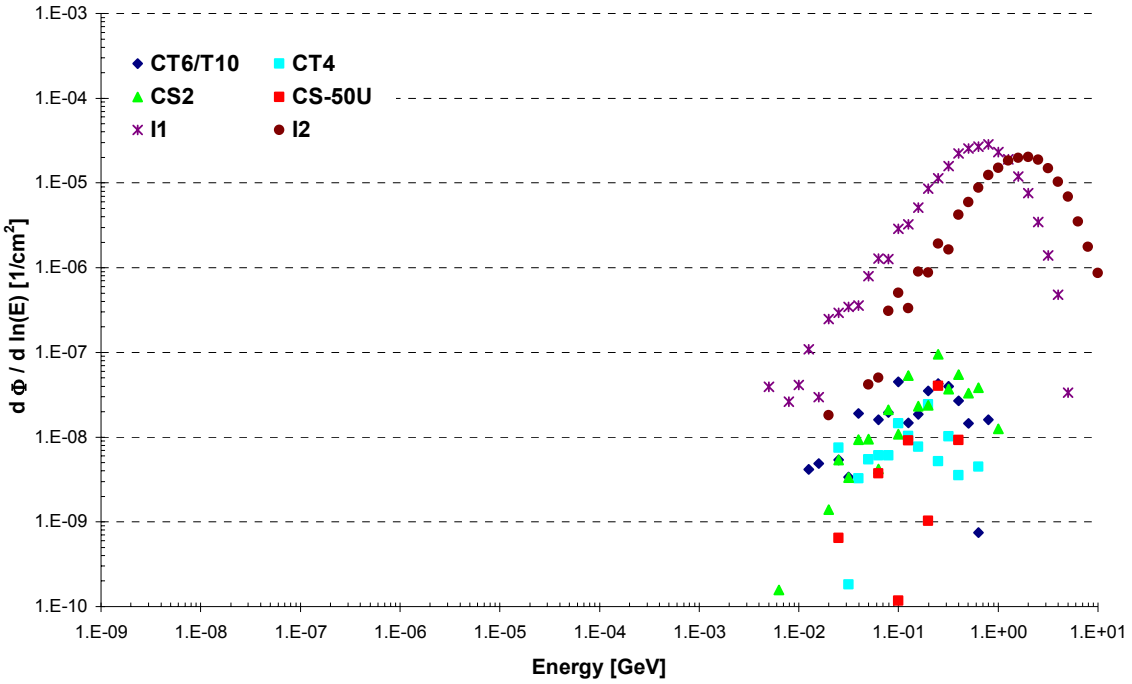

Figure 12 *Kaon fluence spectra for various measurement locations at CERF (lethargy representation). The error bars were omitted for clarity*

Comparison of the geometry models

Figures 13 – 19 show the fluence spectra obtained with the accurate and the simple geometry implementation for the CERF reference position CT6/T10. As a result it can be seen that the simplified model yields results of high statistical significance.

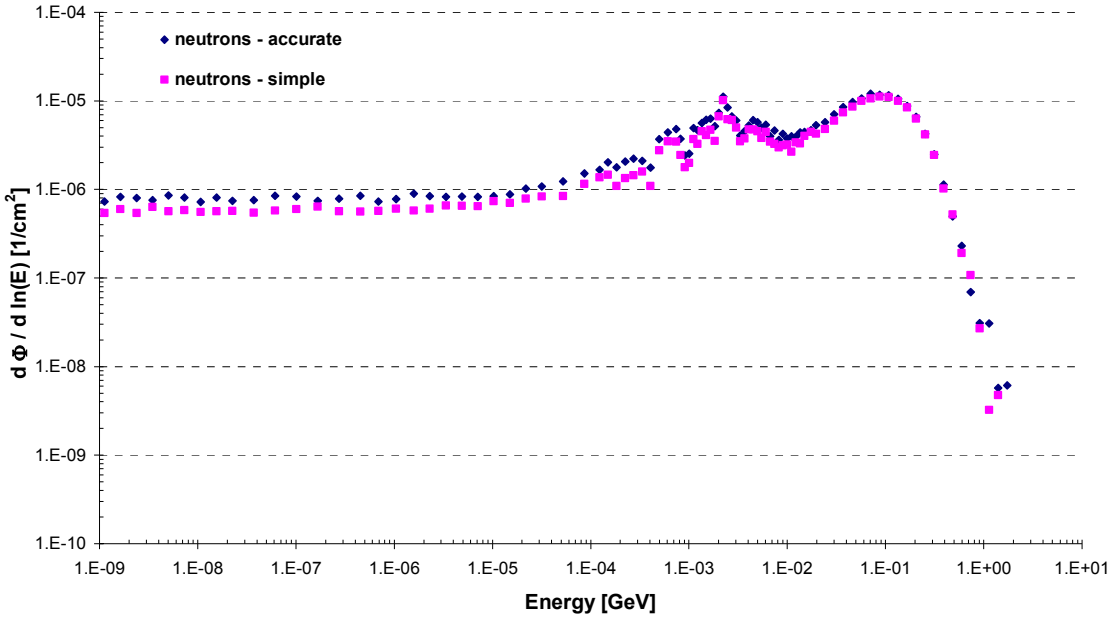

Figure 13 *Neutron fluence spectra obtained from the accurate and the simplified geometry model (lethargy representation). The error bars were omitted for clarity.*

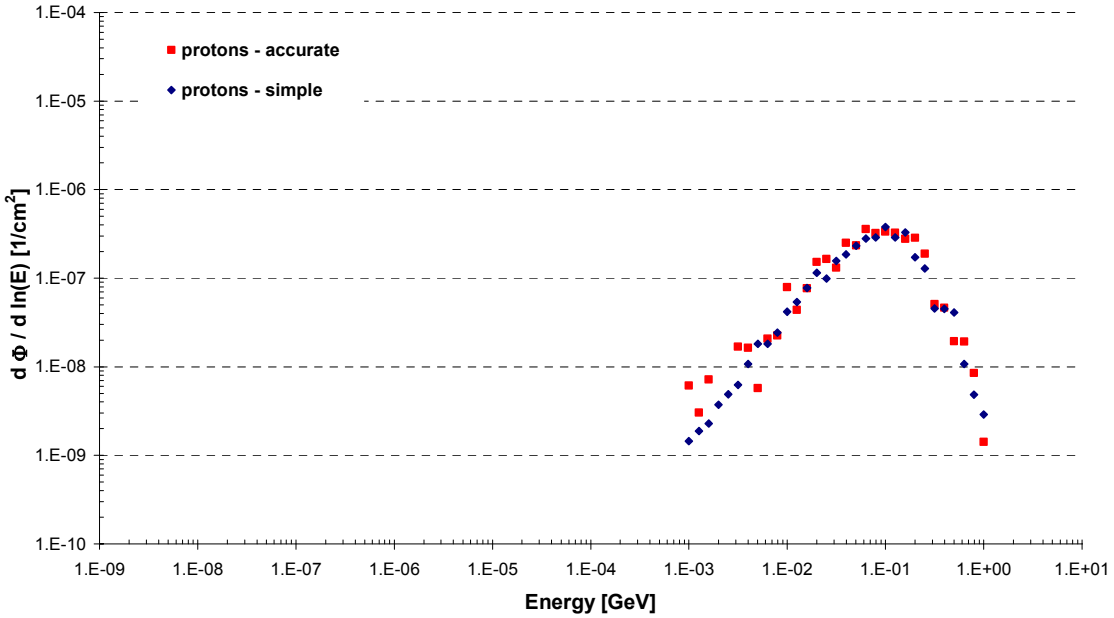

Figure 14 *Proton fluence spectra obtained from the accurate and the simplified geometry model (lethargy representation). The error bars were omitted for clarity.*

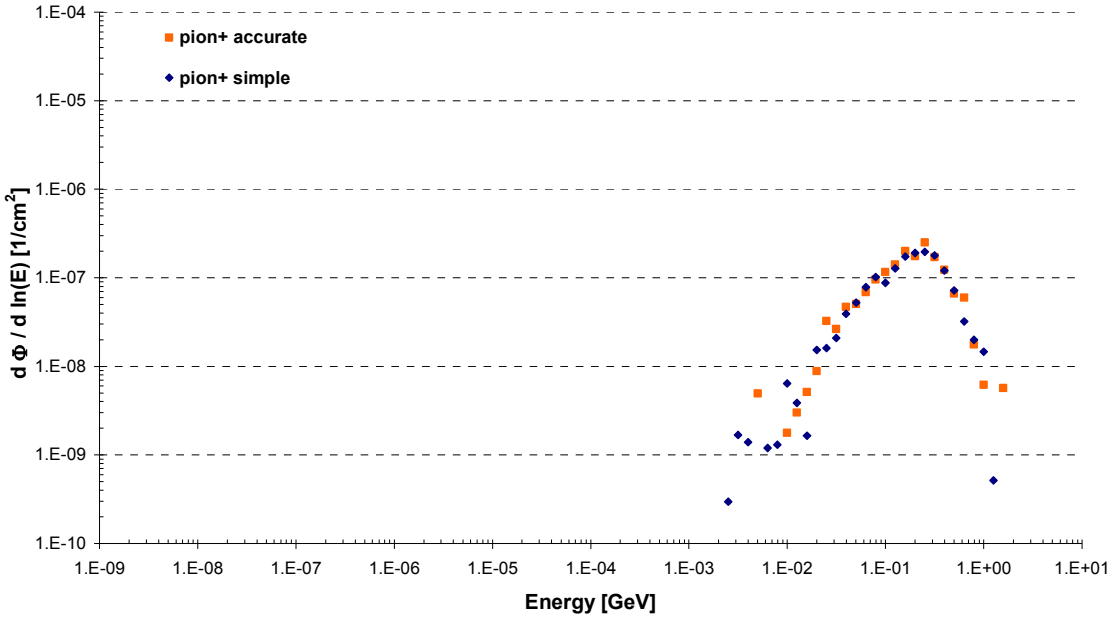

Figure 15 *Pion^{+} fluence spectra obtained from the accurate and the simplified geometry model (lethargy representation). The error bars were omitted for clarity.*

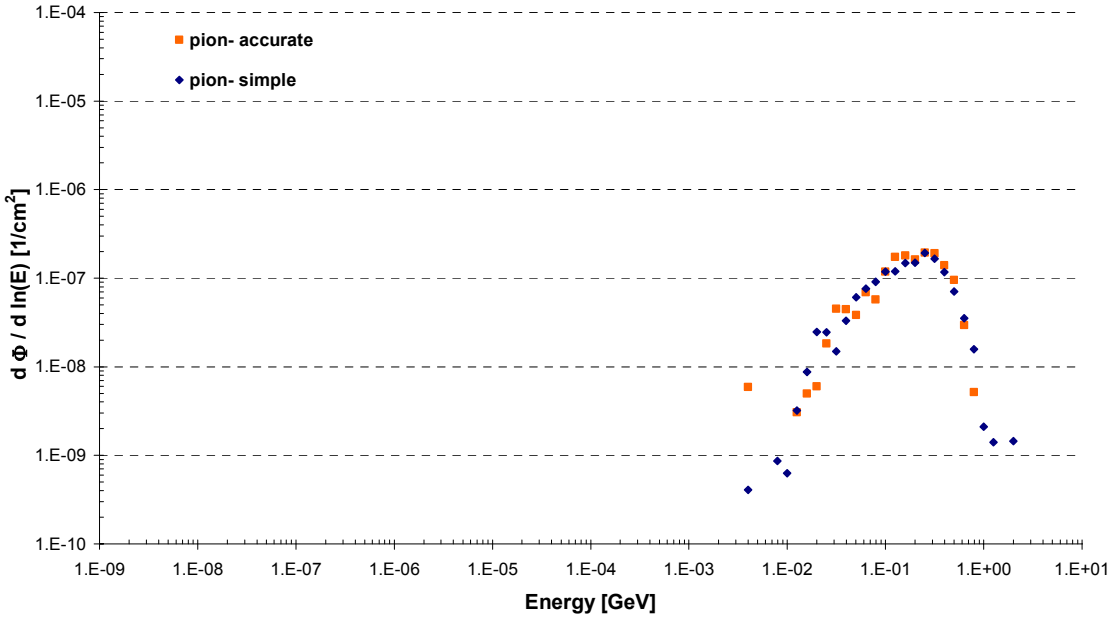

Figure 16 *Pion^{-} fluence spectra obtained from the accurate and the simplified geometry model (lethargy representation). The error bars were omitted for clarity.*

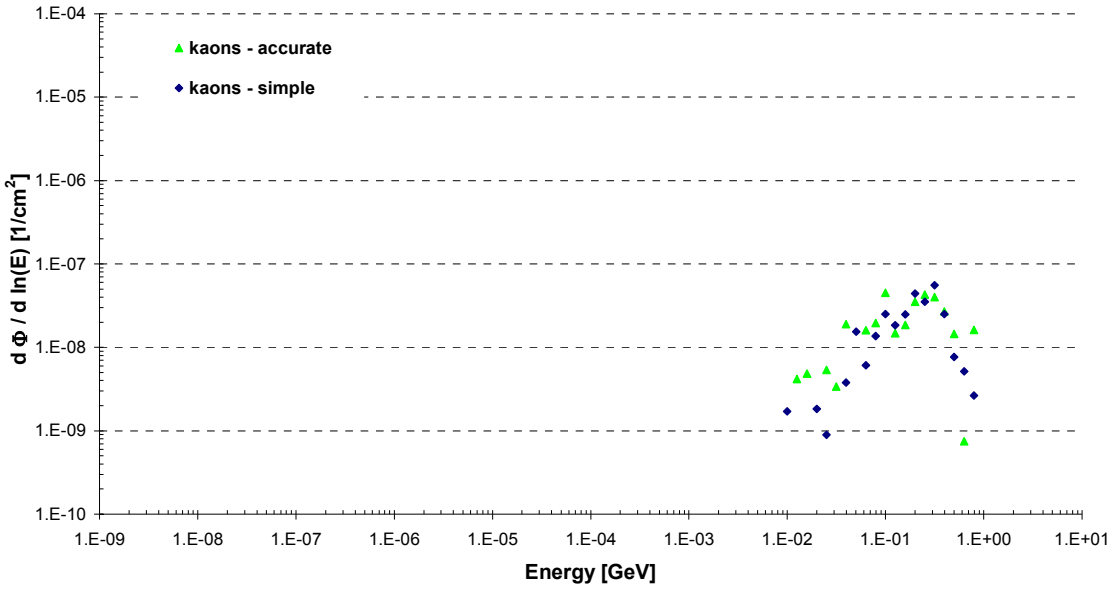

Figure 17 *Kaon fluence spectra obtained from the accurate and the simplified geometry model (lethargy representation). The error bars were omitted for clarity.*

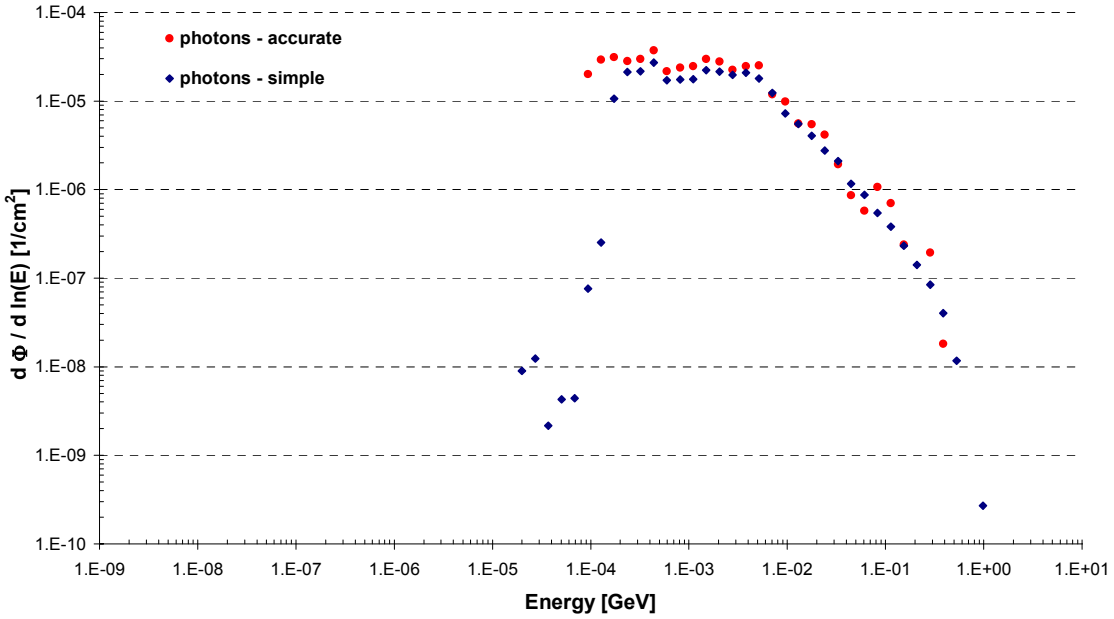

Figure 18 *Photon fluence spectra obtained from the accurate and the simplified geometry model (lethargy representation). The error bars were omitted for clarity.*

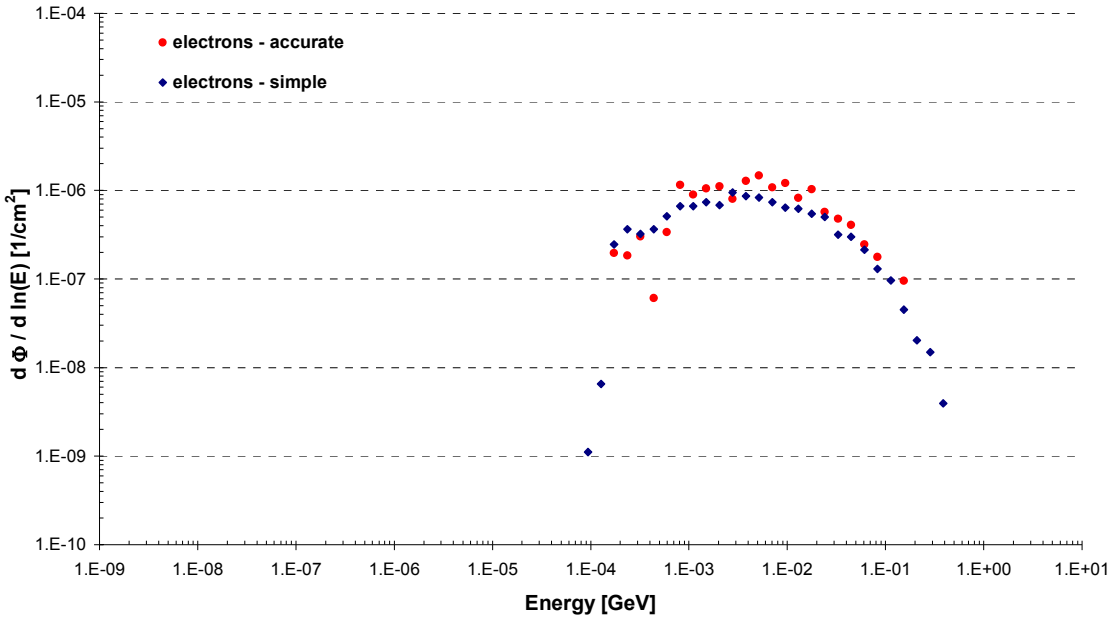

Figure 19 *Electron fluence spectra obtained from the accurate and the simplified geometry model (lethargy representation). The error bars were omitted for clarity.*